INFECTION AND IMMUNITY, July 2000, p. 4245–4254 Vol. 68, No. 7
0019-9567/00/$04.00+0

Genetic Locus for Streptolysin S Production by Group A Streptococcus

VICTOR NIZET,[1] BERNARD BEALL,[2] DARRIN J. BAST,[3] VIVEKANANDA DATTA,[1] LAURIE KILBURN,[3] DONALD E. LOW,[3] AND JOYCE C. S. DE AZAVEDO[3]*

Department of Pediatrics, Division of Infectious Diseases, University of California, San Diego, La Jolla, California 92093[1]; Centers for Disease Control and Prevention, National Center for Infectious Diseases, Respiratory Diseases Branch, Atlanta, Georgia 30333[2]; and Department of Microbiology, Mount Sinai Hospital and University of Toronto, Toronto, Ontario, Canada M5G 1X5[3]

Received 17 February 2000/Returned for modification 9 March 2000/Accepted 23 March 2000

Group A streptococcus (GAS) is an important human pathogen that causes pharyngitis and invasive infections, including necrotizing fasciitis. Streptolysin S (SLS) is the cytolytic factor that creates the zone of beta-hemolysis surrounding GAS colonies grown on blood agar. We recently reported the discovery of a potential genetic determinant involved in SLS production, *sagA*, encoding a small peptide of 53 amino acids (S. D. Betschel, S. M. Borgia, N. L. Barg, D. E. Low, and J. C. De Azavedo, Infect. Immun. 66:1671–1679, 1998). Using transposon mutagenesis, chromosomal walking steps, and data from the GAS genome sequencing project (www.genome.ou.edu/strep.html), we have now identified a contiguous nine-gene locus (*sagA* to *sagI*) involved in SLS production. The *sag* locus is conserved among GAS strains regardless of M protein type. Targeted plasmid integrational mutagenesis of each gene in the *sag* operon resulted in an SLS-negative phenotype. Targeted integrations (i) upstream of the *sagA* promoter and (ii) downstream of a terminator sequence after *sagI* did not affect SLS production, establishing the functional boundaries of the operon. A rho-independent terminator sequence between *sagA* and *sagB* appears to regulate the amount of *sagA* transcript produced versus transcript for the entire operon. Reintroduction of the nine-gene *sag* locus on a plasmid vector restored SLS activity to the nonhemolytic *sagA* knockout mutant. Finally, heterologous expression of the intact *sag* operon conferred the SLS beta-hemolytic phenotype to the nonhemolytic *Lactococcus lactis*. We conclude that gene products of the GAS *sag* operon are both necessary and sufficient for SLS production. Sequence homologies of *sag* operon gene products suggest that SLS is related to the bacteriocin family of microbial toxins.

Group A streptococcus (GAS), specifically *Streptococcus pyogenes*, is a common cause of pharyngitis, impetigo, and many other human respiratory tract and soft tissue infections. Recently, there has been a dramatic increase in reports of severe invasive GAS infections, including necrotizing fasciitis and toxic shock syndrome (44). Although GAS produces a wide array of virulence factors, those responsible for the rapid bacterial spread and tissue injury seen with invasive GAS infections are unknown.

A hallmark feature of GAS in the clinical laboratory is the zone of beta-hemolysis observed surrounding colonies grown on the surface of blood agar media. The factor responsible for the beta-hemolytic phenotype is streptolysin S (SLS), the oxygen-stable cytolytic toxin of GAS. Despite detailed investigations over several decades, the exact chemical nature of SLS has remained a great mystery of GAS biology. SLS can exist in intracellular, cell-surface-bound, and extracellular forms (16), but attempts at purification are complicated by instability of the cytolytic activity in the absence of high-molecular-weight carriers, such as yeast RNA core or albumin (47).

We have adopted a molecular genetic approach towards the identification of SLS and the study of its contribution to disease pathogenesis. Recently, we reported that Tn*916* mutagenesis of two GAS clinical isolates yielded mutants with an SLS-negative phenotype (8). The single transposon insertion in each mutant mapped to a promoter motif just upstream of a unique open reading frame (ORF), encoding a 53-amino-acid (aa) peptide, which we named *sagA* (SLS-associated gene). In contrast to the parent strains, these SLS-deficient transposon mutants were incapable of inducing necrotic lesions in a mouse model of subcutaneous infection, establishing SLS as a potential GAS virulence factor.

In the present study, we have used Tn*917* mutagenesis, chromosomal walking steps, and data from the University of Oklahoma GAS genome sequencing project (www.genome.ou.edu/strep.html) to discover eight additional ORFs (*sagB* to *sagI*) situated immediately downstream of *sagA* in an operon structure. Targeted plasmid integrational mutagenesis was used to probe the requirement of each gene for SLS production and to define the functional boundaries of the *sag* locus. A recombinant plasmid containing the nine-gene *sag* operon was sufficient for complementation and heterologous expression of the SLS phenotype in *Lactococcus lactis*. Sequence analysis of the *sag* locus gene products suggests that SLS is related to the bacteriocin family of microbial toxins, which are genetically encoded by an operon including the structural (prepropeptide) gene and genes required for the chemical modification, processing, and export of the mature form.

MATERIALS AND METHODS

Bacterial strains, culture conditions, and transformation. Bacterial strains used in this study are listed in Table 1. GAS strain NZ131 is a T14/M49 isolate from a patient with acute poststreptococcal glomerulonephritis that produces SLS and streptolysin O (SLO), streptokinase, DNase, and pyrogenic exotoxin (SPE) B (42). GAS were grown in Todd-Hewitt broth (THB) or on Trypticase soy agar + 5% sheep's blood (SBA). For antibiotic selection, 2 μg of erythromycin (EM) or chloramphenicol (CM) per ml was added to the media. *Escherichia coli* strains DH5α and DH10B were grown in Luria-Bertani broth or on

* Corresponding author. Mailing address: Department of Microbiology, Room 1483, Mount Sinai Hospital, 600 University Ave., Toronto, Canada M5G 1X5. Phone: (416) 586-8459. Fax: (416) 586-8746. E-mail: jdeazavedo@mtsinai.on.ca.

TABLE 1. Bacterial strains and plasmids used in this study

Test	Bacterial strain or plasmid	Description	Reference or source
None	Bacteria		
	GAS, NZ131	T14/M49 clinical isolate from patient with glomerulonephritis, SLS^+, SLO^+, streptokinase$^+$, DNase$^+$, SPE B^+	42
	E. coli		
	DH5α	*endA1 hsdR17* ($r_k^-m_k^+$) *supE44 thi-1 recA1 gyrA* (Nal^r) *relA1* Δ(*lacZYA-argF*) U169 ϕ80*dlac* Δ(*lacZ*)M15	50
	DH10B	F^- *mcrA* Δ(*mrr-hsdRMS-mcrBC*) ϕ80*dlac* Δ(*lacZ*)M15 Δ*lacX74 deoR recA1 endA1 araD139* D(*ara*,*leu*)*7697 galU galK* λ^- *rps*L *nup*G	17
	L. lactis NZ9000	MG1363 (lacking nisin operon); *pepN*::*nisRK*	30
Plasmids			
Tn*917* mutagenesis	pTV_1OK	*repA*(Ts)-pWV01Ts *aphA3* Tn*917*(*erm*)	20
	pUC19	*lacZ*α *bla*	Pharmacia
	pSLSneg	pUC19 + chromosome junction of Tn*917* in SLS-negative NZ131 mutant, encompassing *erm* gene	This study
Chromosome walking	pACYC184	*rep*(p15A), Cm^r, Tet^r	38
	pSagB′	pACYC184 + 484-bp intragenic fragment *sagB*	This study
	pFW12	pSF152 derivative, *aad9 spcR* determinant, no gram-positive origin	37
	pSagB-spc	pSagB′ + Spc^r determinant from pFW12	This study
	pSLSup	pSagB-spc + ~7,800 bp upstream NZ131 DNA from *Eco*RI digest of SLS-minus pSagB-spc Campbell insertion mutant, self ligation	This study
	pSLSdown	pSagA-erm + ~7,200 bp downstream NZ131 DNA from partial *Bcl*I digest of allelic exchange mutant, self ligation	This study
Targeted mutagenesis	pCR2.1-topo	ColE *ori*, Amp^r, Kn^r, *lacZ*α	Invitrogen
	pVE6007Δ	Temperature-sensitive derivative of pWV01, Cm^r	34
	p*sag*A.KO	pVE6007Δ + intragenic PCR fragment of *sagA* (codons 2–48)	This study
	p*sag*B.KO	pVE6007Δ + intragenic PCR fragment of *sagB* (codons 39–161)	This study
	p*sag*C.KO	pVE6007Δ + intragenic PCR fragment of *sagC* (codons 225–318)	This study
	p*sag*D.KO	pVE6007Δ + intragenic PCR fragment of *sagD* (codons 141–215)	This study
	p*sag*E.KO	pVE6007Δ + intragenic PCR fragment of *sagE* (codons 47–137)	This study
	p*sag*F.KO	pVE6007Δ + intragenic PCR fragment of *sagF* (codons 56–163)	This study
	p*sag*G.KO	pVE6007Δ + intragenic PCR fragment of *sagG* (codons 21–135)	This study
	p*sag*H.KO	pVE6007Δ + intragenic PCR fragment of *sagH* (codons 28–149)	This study
	p*sag*I.KO	pVE6007Δ + intragenic PCR fragment of *sagI* (codons 116–280)	This study
	p*sag*Up.KO	pVE6007Δ + 291 bp PCR fragment upstream of *sagA* promoter	This study
	p*sag*Down.KO	pVE6007Δ + 241 bp PCR fragment downstream of *sagI* terminator	This study
	pFW15	pSF152 derivative, *ermAM*	37
Complementation analysis and heterologous expression	pDC123	*E. coli*/streptococcal shuttle vector, JS-3 replicon, Cm^r	9
	pSagLocus	pDC123 + 9,440-bp PCR amplicon of entire nine-gene *sag* operon	This study

Luria-Bertani agar; antibiotic selection utilized 100 μg of ampicillin (AMP) per ml, 130 μg of spectinomycin (SPC) per ml, 300 μg of EM per ml, or 5 μg of CM per ml. *L. lactis* NZ900 was grown in M17 broth (Difco) supplemented with 1% glucose (GM17) or on SBA plates, with selection at 5 μg of CM per ml. GAS strains were rendered competent for transformation by growth in THB media plus 0.3% glycine as described for *Streptococcus agalactiae* (13). *L. lactis* was made competent for transformation by growth in GM17 plus 2.5% glycine (22). Plasmids were introduced by electroporation (Eppendorf 2510, 1,500 V), with recovery in THB plus 0.25 M sucrose (GAS) or GM17 media plus 20 mM $MgCl_2$ plus 2 mM $CaCl_2$ (*L. lactis*) for 1 to 2 h prior to antibiotic selection on agar media.

Tn*917* mutagenesis and cloning of transposon insertion site. Mutagenesis of NZ131 with Tn*917* was performed as described for *Streptococcus mutans*, by using the temperature-sensitive delivery vector pTV_1OK (20). The chromosome junction site of the Tn*917* insertion in the single nonhemolytic mutant discovered on SBA screening was cloned as a *Hin*dIII fragment encompassing the transposon *erm* gene into pUC19, selecting for Amp^r and Em^r in the *rpsL* mutant *E. coli* strain DH10B. The resultant plasmid was named pSLSneg.

Chromosome walking steps. A 484-bp PCR fragment was amplified from within *sagB*, was digested with *Eco*RV and *Hin*dIII, and was cloned into *Xmn*I/*Hin*dIII-digested pACYC184, resulting in pSagB′. Subsequently, the Spc^r determinant from pFW12 was cloned into *Eco*RI/*Xmn*I-digested pSagB′ as a compatible *Hin*cII-*Eco*RI fragment, resulting in pSagB-spc. NZ131 was transformed with the nonreplicative plasmid pSagB-spc, and Spc^r colonies exhibited an SLS-negative phenotype. Chromosomal DNA was isolated from the NZ131:pSagB-spc mutant, digested with *Eco*RI, self-ligated, and used to transform *E. coli* strain DH10B to Spc^r. This step resulted in the cloning of ~7,600 bp of additional DNA upstream of *sagB* (pSLSup). To complete *sagH* and identify downstream sequence, NZ131:sagA.Erm (see below) chromosomal DNA was partially digested with *Bcl*I, was self-ligated, and was used to transform *E. coli* DH10B to Erm^r. The resulting plasmid purified from an *E. coli* transformant was termed pSLSdown.

Southern analysis. Total cellular DNA was isolated (31) from NZ131 and 11 additional GAS strains representing a spectrum of *emm* types (4). The genotyped strains, obtained from recent epidemiologic investigations at the Centers for Disease Control and Prevention were 2109/98(*st*2974), 4356/99(*emm*3), 1603/99(*emm*76), 1143-99(*emm*11), 159-99(*emm*28), 134/98(*st*2967), 4315/99(*emm*1), 1489/99(*emm*75), 317/98(*emm*59), 1630/99(*pt*4245), and 3466/99(*emm*5). DNA was digested to completion with *Spe*I, was separated by 0.6% Tris-acetate-EDTA (TAE)-agarose gel electrophoresis, and was transferred to a nylon filter by the Southern method. A digoxigenin-labeled probe of a PCR amplicon comprising *sagD* to *sagF* was prepared by using a Genius Kit (Boehringer Mannheim). The probe was hybridized to the target filter under standard conditions, and the probe-positive bands were visualized by chemiluminescence.

Targeted plasmid integrational mutagenesis. PCR with specific primer pairs (Table 2) was used to amplify intragenic fragments from *sag* genes, as well as fragments from upstream of the *sagA* promoter and downstream of the terminator following *sagI*. PCR products were recovered by T-A cloning in the vector pCR2.1-TOPO (Invitrogen) and then were cloned by *Hin*dIII/*Xba*I digestion in the temperature-sensitive vector pVE6007Δ (34). The resultant knockout plasmids (Table 1) were introduced into NZ131 by electroporation, and Cm^r transformants were identified at the permissive temperature for plasmid replication (30°C). Single-crossover Campbell-type chromosomal insertions were selected by shifting to the nonpermissive temperature (37°C) while maintaining CM selection (52). SLS phenotype was determined on SBA plus CM at 37°C. The fidelity

TABLE 2. Specific *sag* locus PCR primer sets used in the experiments described

Targeted mutagenesis		RT-PCR analysis	
Primer[a]	Sequence	Primer[a]	Sequence
*sag*Up		*SagAB*	
Fwd	5′-GGCCCAAGAACGGAGTGTAT-3′	Fwd	5′-CGGAAGTTATACGCCAGGTA-3′
Rev	5′-GTAGCACGAAAATTCGCTCG-3′	Rev	5′-AGTTATTGGCGGACAATTCT-3′
sagA		*sagBC*	
Fwd	5′-GTGTAGCTGAAACAACTCAAGT-3′	Fwd	5′-AAACGTTAGAGATTTTGCGG-3′
Rev	5′-TATAACTTCCGCTACCACCTTG-3′	Rev	5′-CCTTAACCAACTGTGAAACTAT-3′
sagB		*sagCD*	
Fwd	5′-CCATCATCAAACGGTGCTAA-3′	Fwd	5′-AGCGAAGCTTTCATTATTGC-3′
Rev	5′-CTAATTGATGCTTGTGAACT-3′	Rev	5′-CTTGACTCAACTCACCTATAAATTG-3′
sagC		*sagDE*	
Fwd	5′-ACACTTGTACTTTGAATCCT-3′	Fwd	5′-AGGCCTTTGAACCTTTGATT-3′
Rev	5′-ATATCTTGGACCTGAATCTC-3′	Rev	5′-CAGAGTTGCTCTTAGAAAACCAATT-3′
sagD		*sagEF*	
Fwd	5′-GCGATAAAATGGTAACTGAG-3′	Fwd	5′-TGCTTTAAATCACTTATTGATGGGG-3′
Rev	5′-CGATCTGGATGTATTCAATC-3′	Rev	5′-AAAAAGGTCAGAACCTCTCCTAGA-3′
sagE		*sagFG*	
Fwd	5′-TTTATGACATTTTGGCTTTG-3′	Fwd	5′-TGGGATAGTCAAGGCTTGTC-3′
Rev	5′-AAACGATAAATCGTCTCTTC-3′	Rev	5′-TCTTTTGGGATTGCCCTAAA-3′
sagF		*sagGH*	
Fwd	5′-TTGTTTTATTCTTTTACTCA-3′	Fwd	5′-ACTGGAAAAACGTTACGTTG-3′
Rev	5′-CTTGTTAGCGACTGTTCTCC-3′	Rev	5′-GACTGTTGTCGCAGTATTAAAACTT-3′
sagG		*sagHI*	
Fwd	5′-TGATGTTTCCTTGTCTATTG-3′	Fwd	5′-GCATCCAATACTATTATTCC-3′
Rev	5′-AGAATTGACTTGGAAACTGC-3′	Rev	5′-TTGTTTTGCTTTAGTTGAGC-3′
sagH			
Fwd	5′-CAATTTTGATGATCGTTATT-3′	T7 primer	5′-GTAATACGACTCACTATAGGGC-3′
Rev	5′-CTAGAGGATCCCCCTAAATG-3′		
sagI			
Fwd	5′-TTGACAGACCGATCACGTAG-3′		
Rev	5′-TCCAATCAGCAGGCCAAAGC-3′		
*sag*Down			
Fwd	5′-TGATTGCGATGTTACTGTTG-3′		
Rev	5′-CCCTGATAGCGAACAAGACA-3′		

[a] Fwd, forward; Rev, reverse.

of site-directed recombination events was confirmed by PCR. Confirmed intragenic plasmid integrational mutants were designated NZ131:*sagA*.KO, NZ131:*sagB*.KO, etc. (Fig. 1). The targeted integrations upstream and downstream of the *sag* locus were designated NZ131:*sag*Up.KO and NZ131:*sag*Down.KO, respectively. An SLS-negative allelic replacement mutant of *sagA* in NZ131 was also constructed. In this mutant, NZ131.*sagA*::Erm, the *sagA* gene was replaced with a *sagA* derivative containing the nonreplicative plasmid bearing Em^r, pFW15 (U50977), inserted in the *Spe*I site.

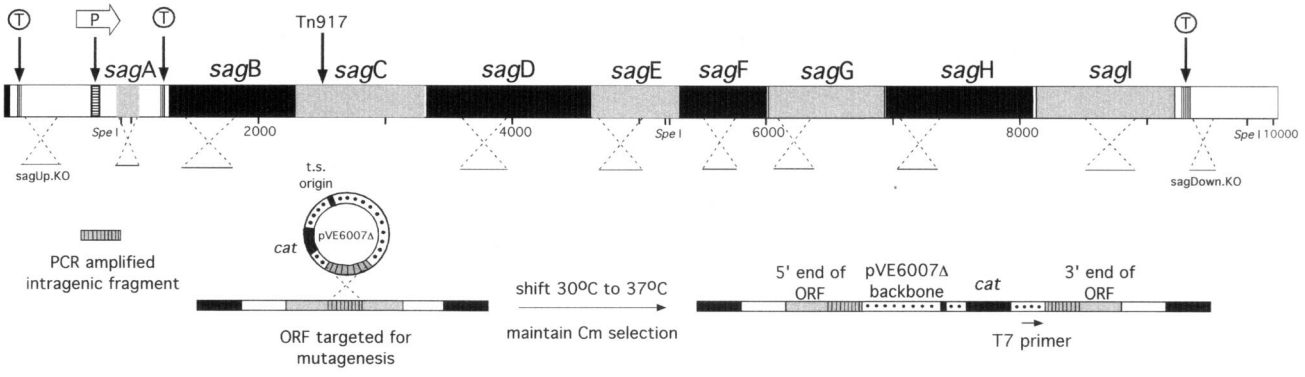

FIG. 1. Map of the *sag* genetic locus required for SLS production by GAS. Loci targeted for mutagenesis are also shown.

TABLE 3. Predicted protein products of genes in the GAS *sag* locus[a]

Gene	Protein length (aa)	Protein mass (kDa)	PSORT localization	Homology	Similar protein	% Identity (% similarity)
sagA	53	5.2		Bacteriocin	*E. coli* McbA	
	23			Leader peptide	Leader	39 (52)
	30*	2.9*		Prepropeptide	C-terminal region	37 (57)*
sagB	316	36.0	Cytoplasm	Modifying enzyme	*E. coli* McbB	23 (42)
sagC	352	40.3	Membrane	None		
sagD	452	51.6	Cytoplasm	None		
sagE	223	25.4	Membrane	Immunity protein	*L. plantarum* PlnP	24 (52)
sagF	227	26.2	Membrane	None		
sagG	307	34.2	Membrane	ABC transporter	*B. subtilis* YfiL	47 (63)
sagH	375	42.2	Membrane	ABC transporter	*B. subtilis* YfiM	19 (39)
sagI	372	41.7	Membrane	ABC transporter	*B. subtilis* YfiN	24 (47)

[a] *, propeptide portion of SagA with cleavage of leader peptide at GG site.

Transcriptional analysis. For Northern blots, a 30-ml culture of GAS was grown for 2 to 4 h post-mid-log phase (optical density at 600 nm, 0.8 to 1.2). Bacteria were pelleted and resuspended in Trizol reagent (Gibco) and were transferred to Fast RNA tubes with matrix (BIO101), and RNA was isolated by using the FASTPREP machine (BIO101) for 23 s at a speed setting of 6.0. RNA (3 or 15 μg) was electrophoresed on a 1.2% formaldehyde denaturing gel and was transferred to a nylon membrane (Hybond N^+; Amersham) by standard methods. Membranes were incubated with digoxigenin-labeled (Boehringer Mannheim) *sagA* or *sagB* probe overnight at 50°C. Chemiluminescent detection was performed by using an anti-digoxigenin-alkaline phosphatase conjugate and autoradiography according to the manufacturer's instructions.

For reverse transcriptase PCR (RT-PCR) analysis, total RNA was prepared from GAS harvested 2 to 4 h post-mid-log phase. Bacterial pellets were lysed by using Tris-EDTA buffer containing lysozyme (3 mg/ml) and mutanolysin (10 mg/ml), and total RNA was isolated by using the RNeasy miniprotocol (QIAGEN). RNA samples were digested for 15 min at 25°C with 1 U of RNase-free DNase (Gibco) per ml to remove contaminating DNA. Reverse transcription was performed by using the Calypso RT-PCR system (DNAmp Ltd.) with specific paired *sag* gene primers (Table 2) or the T7 primer sequence of pVE6007Δ. Control reactions using the same paired primers prior to reverse transcription were used to confirm the absence of contaminating chromosomal DNA.

Complementation analysis and heterologous expression of SLS in *L. lactis*. A 9,440-bp amplicon comprising the entire nine-gene *sag* locus was amplified by using the high fidelity Expand Long Template PCR System (Boehringer Mannheim) according to the manufacturer's instructions. The amplicon sequence, from ~600 bp upstream of the *sagA* promoter motif to ~300 bp downstream of the terminator motif behind *sagI*, was captured by T-A cloning in the vector pCR2.1-TOPO (Invitrogen). The complete *sag* locus DNA was then directionally cloned as a *Bam*HI/*Apa*I fragment into the shuttle vector pDC123 (9) cut with the same enzymes. The resultant plasmid, pSagLocus, was used to transform the nonhemolytic *sagA* allelic exchange mutant NZ131.*sagA*::Erm, with selection for Em^r and Cm^r. For the heterologous expression study, pSagLocus was used to transform nonhemolytic *L. lactis* NZ9000 with selection for Cm^r. In each case, control transformations were performed with vector pDC123 alone.

Nucleotide sequence accession number. All new sequence data from the present study have been submitted to the DDBJ/EMBL/GenBank databases under the accession numbers AF067723, AF067649, and AF163682.

RESULTS

Tn*917* mutagenesis and discovery of downstream *sag* genes. One of 1,200 Tn*917* mutant colonies of GAS strain NZ131 exhibited an SLS-negative phenotype when screened on SBA. The Tn*917* insertion site in this mutant was cloned in pUC19 to produce pSLSneg. Sequence analysis of pSLSneg with primers annealing to Tn*917* and pUC19 revealed a 660-bp fragment of the NZ131 chromosome with 100% sequence identity to an ORF with a contiguous sequence (contig) from the ongoing M1 GAS genome project and served as a starting point for the discovery of the apparent *sag* operon.

Chromosome walking and DNA sequence linkages yield extended *sag* locus. The complete *sag* locus was deduced from a compilation of sources: (i) sequencing of the previously reported 3.8-kb *Hin*dIII fragment from the M1 GAS strain MGAS166 containing *sagA* (8); (ii) sequencing of pSLSneg containing the chromosomal insertion site of Tn*917* (within *sagC*) in the SLS-negative NZ131 mutant described above; (iii) chromosomal walking steps in which plasmid recovery from SLS-negative Campbell insertion mutants captured additional sequence information; and, importantly, (iv) discovery of homology with two contigs in the ongoing M1 GAS sequencing project at the University of Oklahoma. All *sag* ORFs identified from the M1 sequencing project data were confirmed to be present in M49 GAS strain NZ131 by PCR amplification and the targeted mutagenesis experiments described below.

The ORF disrupted by Tn*917* in NZ131 was ultimately recognized as *sagC*. Examination of the M1 genome project contig to which it had 100% homology revealed one upstream ORF (*sagB*), and four complete downstream ORFs (*sagD* to *sagG*), ending with a truncated ORF (start of *sagH*). Chromosome walking upstream was achieved by plasmid integrational mutagenesis of *sagB*, followed by restriction digestion of the mutant chromosomal DNA, self ligation, transformation of *E. coli*, and recovery of the plasmid pSLSup. Sequence analysis of pSLSup revealed the overlap with our previously published 53-codon ORF *sagA*, as well as a potential rho-independent terminator between *sagA* and *sagB*. Chromosome walking downstream was achieved by plasmid integrational mutagenesis of *sagA*, partial restriction digestion of the mutant chromosomal DNA, self ligation, transformation of *E. coli*, and recovery of the plasmid pSLSdown. Sequence analysis of pSLSdown with a primer annealing to the truncated *sagH*, followed by a BLAST search against the M1 database, revealed sequence identity to the end of a third contig. The sequence from this contig provided the completion of *sagH*, followed immediately downstream by another ORF (*sagI*), and, 50 bp further downstream, a motif resembling a rho-independent terminator.

Sequence analysis of the *sag* locus genes. Figure 1 shows the genetic structure of the nine-gene *sag* locus, including pro-

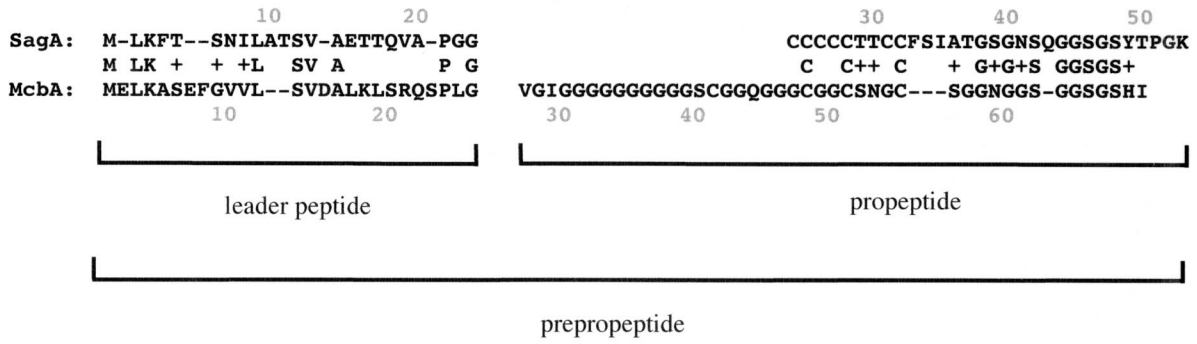

FIG. 2. Amino acid sequence similarity between SagA and McbA of *E. coli*.

moter and terminator motifs, while Table 3 lists the ORF size, predicted protein mass, PSORT prediction, and GenBank homologies of each identified gene. The *sagA* ORF encodes a 53-aa product with sequence features suggestive of a bacteriocin precursor (prepropeptide). These features include a potential glycine-glycine cleavage site, which would yield leader peptide (23 aa) and propeptide (30 aa) of characteristic size and an abundance of target residues (cysteine, serine, and threonine) known to undergo posttranslational modification. Figure 2 shows similarity between the leader sequences and the C-terminal propeptide regions of the predicted *sagA* gene product with the microcin B17 precursor (McbA) from *E. coli*. Microcin B17, a bacteriocin, is produced by an operon that includes modifying enzymes (McbB to -D) for posttranslational modification of propeptide amino acids and an ATP transporter secretion-immunity apparatus (McbE to -F) (53). The predicted protein product of *sagB* is a 36.0-kDa species likely localized to the cytoplasm that shares weak homology with McbB. A sequence possessing an inverted repeat stem of 17 bp (or 15 bp to allow a loop of 4 bp) followed by 9 nucleotides, 6 of which are Ts, is located between the *sagA* and *sagB* ORFs, consistent with a rho-independent terminator (GTAA TTAGCAGGTACTA. . .GA. . .TAGTACCTGCTAATTAC . . .TATATGTTT).

The predicted protein products SagC (40.3 kDa) and SagF (26.2 kDa) share no homologies with proteins in the GenBank databases. Using the TopPred II 1.2 program, we discovered that SagC has two potential membrane-spanning segments at aa 215 to 230 and at aa 272 to 292. By using the same program, we discovered that SagG has six membrane-spanning regions dispersed across its length and is very hydrophobic in general. Both SagC and SagF are predicted to be membrane proteins by the PSORT localization program. The SagD gene product is a predicted cytoplasmic protein of 51.6 kDa, also without homologies. SagE (25.4 kD) is a possible membrane protein with weak homology to PlnP, a putative *Lactobacillus plantarum* bacteriocin immunity protein (11). SagG (41.7 kDa), SagH (42.2 kDa), and SagI (41.7 kDa) have strong homologies to several known or postulated multicomponent ATP-binding cassette (ABC)-type membrane transporter complexes, in particular YfiL-YfiM-YfiN of *Bacillus subtilis* (51). SagG itself contains the signature patterns for this class of proteins, the Walker A and Walker B motifs (49) in the heart of the ATP-binding pocket. Approximately 50 bp beyond the stop codon of *sagI* lies an apparent rho-independent terminator sequence.

The *sag* locus is conserved across GAS strains of differing serotypes. Recognition sites for restriction enzyme *Spe*I are found within *sagA*, twice within *sagE*, and downstream beyond the *sagI* terminator sequence (Fig. 1). Southern blot analysis was performed on *Spe*I-digested chromosomal DNA from NZ131 and 11 other GAS strains of differing *emm* (M protein gene) types (Fig. 3). When probed with a *sagD* to *-F* PCR

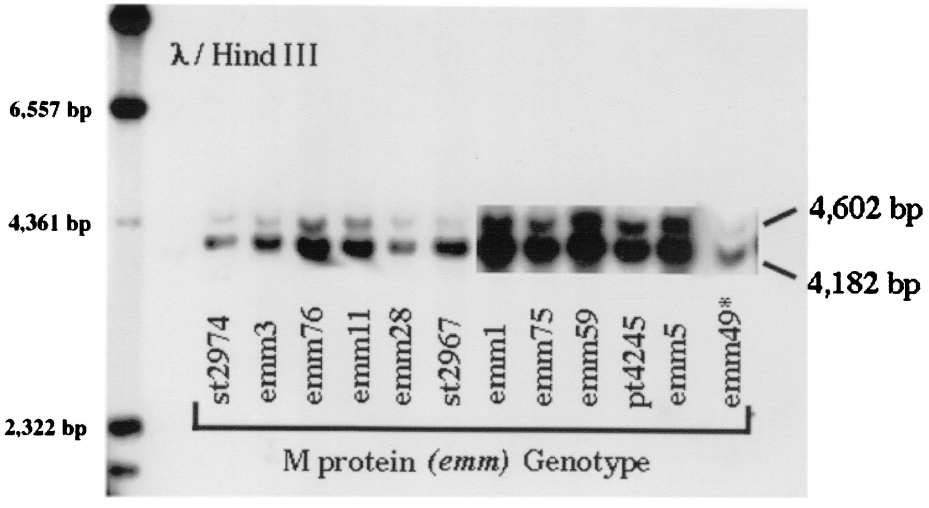

FIG. 3. Southern blot analysis showing the conservation of the *sag* locus among GAS isolates from a variety of *emm* (M protein) genotypes. Blot was probed with a digoxigenin-labeled PCR amplicon encompassing *sag*D to *sag*F.

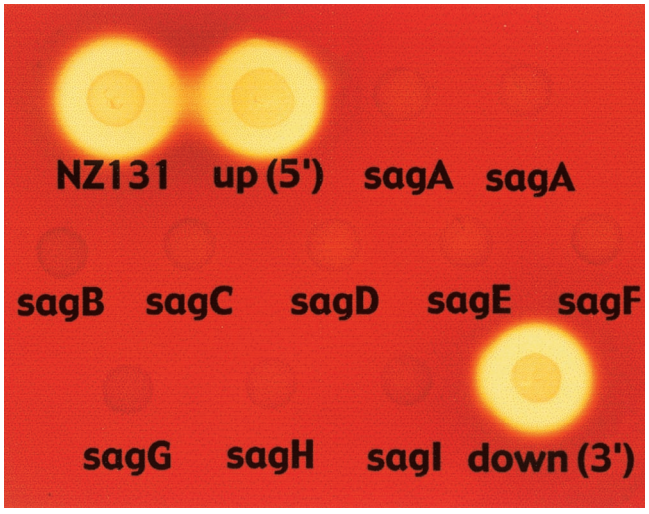

FIG. 4. SLS phenotype following targeted knockouts of *sag* locus genes.

amplicon, two hybridizing bands corresponding to the expected 4,602-bp (*sagA* to *-E*) and 4,182-bp (*sagF* to *-I*) fragments were invariably observed, showing that the *sag* locus is conserved among GAS.

Targeted mutagenesis of *sag* locus genes defines the functional boundaries of the *sag* locus. In order to (i) confirm the requirement of individual *sag* locus genes for SLS expression and (ii) define the functional boundaries of the *sag* locus, a series of targeted plasmid integrational mutants were constructed by using homologous recombination cassettes cloned into a temperature-sensitive suicide vector. Our earlier studies had shown that a random Tn*916* integration that mapped within the *sagA* promoter resulted in an SLS-negative phenotype (8). In the present study, we found that a random Tn*917* integration that mapped to the *sagC* ORF was also associated with loss of SLS expression. Figure 4 shows that targeted plasmid integrational mutagenesis of *sagA*, *sagB*, *sagD*, *sagE*, *sagF*, *sagG*, *sagH*, and *sagI* resulted in NZ131 mutants that invariably failed to produce detectable SLS activity. An SLS-negative double-crossover allelic exchange replacement of *sagA* (NZ131.*sagA*::Erm) was also constructed. Plasmid integrations 300 bp upstream of the *sagA* promoter (*sag*Up.KO) and 50 bp downstream of the apparent rho-independent terminator following *sagI* (*sag*Down.KO) retained the wild-type SLS activity of parent strain NZ131.

Transcription analysis reveals operon structure of GAS *sag* locus. Northern blot analysis (data not shown) revealed that parent strain NZ131 produced an abundant transcript of approximately 450 bp in size which hybridized with *sagA*. This transcript, corresponding to the size predicted from the *sag* promoter to the terminator motif between *sagA* and *sagB*, was absent in the SLS-deficient mutants NZ131:*sagA*.KO and NZ131.*sagA*::Erm. These findings were identical to our earlier observations with M1 GAS parent strains and SLS-negative Tn*916* mutants of the *sag* promoter (8). Northern blot analysis of SLS-negative targeted mutants in downstream genes of the locus (*sagB*.KO through *sagI*.KO) all revealed wild-type levels of the 450-bp *sagA* transcript. Targeted plasmid integration upstream of the *sagA* promoter (*sag*Up.KO) also failed to abolish production of the *sagA* transcript. These findings confirmed the start of transcription at the *sagA* promoter and demonstrated that *sagA* transcript alone is insufficient to produce the SLS phenotype. Multiple attempts at detection of *sagB* transcript by Northern analysis of NZ131 and M1 GAS strains were unsuccessful, even when five times the amount of RNA preparation was analyzed. We have performed dot blot analysis on total RNA from NZ131, which yields very weak but detectable signals of equivalent intensity when probed with downstream genes (*sagB*, *sagC*, and *sagG*), compared to a very strong signal when probed with *sagA* (data not shown). These data suggested that mRNA for downstream genes in the *sag* locus was unstable or was produced in very low abundance.

No additional promoter motifs were found after *sagA*, and the *sagB* ORF begins just 25 bp downstream of the rho-independent terminator sequence. Thus, we hypothesized that downstream genes in the locus also utilized the promoter upstream of *sagA*. This hypothesis was tested by using an RT-PCR approach recently devised for the analysis of long multigene bacterial operons (19). These data showed that RNA encoding *sagB* was encoded on the same transcript as RNA encoding *sagA*, since a product of expected 300 bp size was amplified with specific *sagA* forward and *sagB* reverse primers from wild-type NZ131 (Fig. 5a). Similar RT-PCR analysis revealed that *sagB* transcript was linked to *sagC* (460 bp), *sagC* to *-D* (410 bp), *sagD* to *-E* (408 bp), *sagE* to *-F* (404 bp), *sagF* to *-G* (402 bp), *sagG* to *-H* (430 bp), and *sagH* to *-I* (451 bp), indicating that the *sag* locus represents a nine-gene operon. RT-PCR yielded product bands of similar intensity for each linkage, as would be predicted for a single mRNA transcript, assuming equal efficiency of each primer set.

RT-PCR analysis was also used to assess downstream transcription in two targeted *sag* gene mutants. These mutants had been specifically constructed with an insertional vector that lacked transcriptional and translational terminators and possessed a strong promoter oriented in the 5′→3′ direction to limit polar effects. Transcript was present in mutants NZ131:*sagA*.KO and NZ131:*sagB*.KO possessing 3′ sequence of the insertional vector (forward T7 primer, 65 bp from terminus) and continuing through to sequence from the next gene in the operon (Fig. 5b). The expected products of 467 bp for NZ131:*sagA*.KO (T7 forward to *sagAB* reverse primer) and 1,061 bp for NZ131:*sagB*.KO (T7 forward to *sagBC* reverse primer) were amplified, demonstrating that the targeted mutations are not completely polar.

Reintroduction of the *sag* locus in *trans* restores hemolytic activity to SLS-negative mutant. A 9,440-bp PCR amplicon comprising the entire nine-gene *sag* locus was amplified and

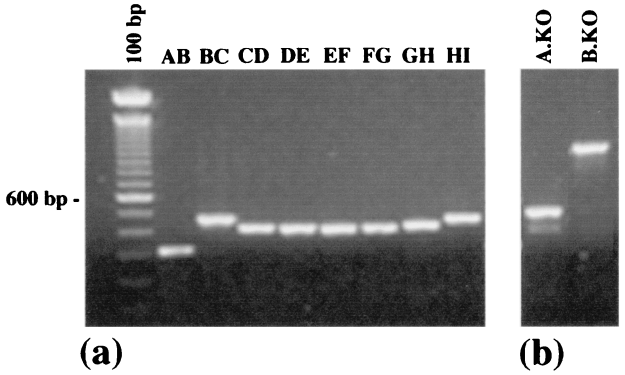

FIG. 5. (a) RT-PCR analysis of total RNA from NZ131. Transcript of predicted size is identified using a *sagA* forward primer and a *sagB* reverse primer, *sagB* forward primer and *sagC* reverse primer, etc. (b) RT-PCR analysis of total RNA from SLS-negative mutants NZ131:*sagA*.KO and NZ131:*sagB*.KO, demonstrating presence of transcript extending from the 3′ end of the integrative vector (T7) to the next gene in the operon.

FIG. 6. Restoration of SLS-activity to the nonhemolytic *sagA* allelic exchange mutant by reintroduction of the nine-gene *sag* operon on a plasmid vector.

cloned in vector pDC123 to yield plasmid pSagLocus. On repeated experiments in which this construct was used to transform the nonhemolytic *sagA* allelic exchange mutant NZ131.*sagA*::Erm, wild-type levels of hemolytic activity were restored (Fig. 6). The pSagLocus-complemented mutants grew more slowly than mutants containing the vector pDC123 alone, suggesting some toxicity with overexpression of the *sag* locus gene products, many of which are predicted integral membrane proteins.

Heterologous expression of the SLS phenotype in *L. lactis*. Plasmid pSagLocus did not confer a beta-hemolytic phenotype to the gram-negative *E. coli* used as an intermediary for cloning. However, when this plasmid was used to transform the nonpathogenic, nonhemolytic gram-positive coccus *L. lactis* NZ9000 (29), a robust and stable beta-hemolytic phenotype was observed in transformants (Fig. 7). The transformed *L. lactis* did not exhibit any other differences from the parent strain on the API-20 system (BioMerieux) for identification of streptococci and related lactic acid bacteria. The presence of the intact pSagLocus in the beta-hemolytic transformants was confirmed by plasmid purification, restriction analysis, and individual PCR amplification of all nine genes. Therefore, the *sag* locus is not only necessary for SLS activity in GAS, it is sufficient to confer the SLS phenotype to a heterologous, nonhemolytic bacterial species. These findings strongly suggest that the *sag* locus encodes the structural determinant for the SLS toxin and any additional genes required for its proper processing and export.

DISCUSSION

SLS is the much studied, yet poorly understood, oxygen-stable and nonimmunogenic beta-hemolysin elaborated by GAS. In addition to the classic lytic effect on sheep erythrocytes, SLS can damage other cell membranes, including those of lymphocytes (23), neutrophils, and platelets (15), certain tissue culture and tumor cells (46), and subcellular organelles such as lysosomes (7) and mitochondria (26). By weight, SLS is one of the most potent cytotoxins known (28). The SLS peptide has never been fully purified nor has the genetic basis of its production been previously elucidated.

In this paper, we present the identification and analysis of a genetic locus (*sagA* to *sagI*) required for SLS activity in GAS. These studies extend and confirm our earlier discovery of the *sagA* gene and its importance for the SLS phenotype (8). Targeted mutagenesis and complementation analysis were used to define the functional boundaries of the *sag* locus, and transcriptional analysis demonstrated its operon structure. Our heterologous expression of a beta-hemolytic phenotype in *L. lactis* demonstrated that genes of the *sag* operon are also sufficient for production of functional SLS. Beta-hemolysis was not observed in *E. coli* transformed with the identical *sag* operon construct. We hypothesize that use of a closely related bacterial species was needed for heterologous expression of SLS because of fundamental differences between the gram-positive and -negative cell walls and the prediction that a number of the *sag* locus genes including the ATP transporter apparatus are membrane-associated. There are no homologies between GAS *sagA* and *-F* genes and known *L. lactis* genes. However, *L. lactis*, like all prokaryotes and eukaryotes studied, possesses ABC-type transporters involved in translocation of substrates (e.g., ions, sugars, amino acids, peptides, and pro-

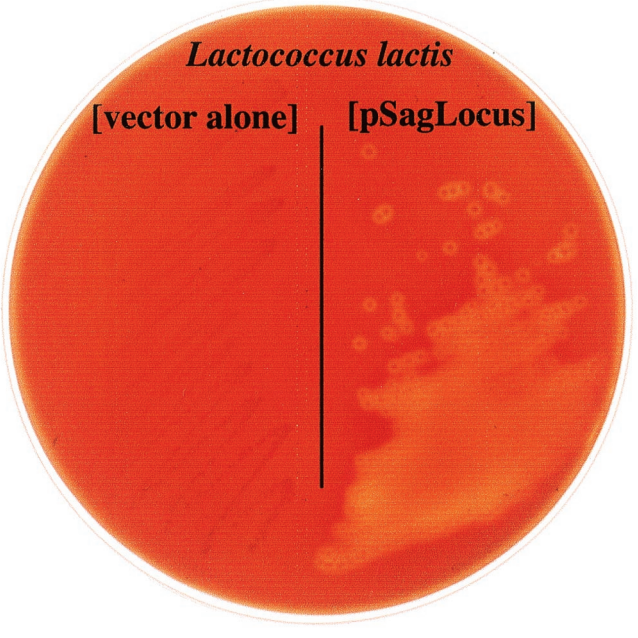

FIG. 7. Plasmid pSagLocus confers beta-hemolytic phenotype to *L. lactis*.

teins) across membranes. Recent precedent for heterologous expression of a multigene streptococcal operon in *L. lactis* exists: introduction of the 13-gene exopolysaccharide synthesis cluster from *Streptococcus thermophilus* into *L. lactis* resulted in production of an altered polysaccharide capsule (45).

Our Southern analysis demonstrates that the *sag* locus is conserved among GAS strains regardless of serotype. Failure of targeted mutagenesis upstream of the *sagA* promoter and downstream of the *sagI* terminator to affect SLS production defines the functional boundaries of the locus. Inactivation of each and every gene in the locus results in an SLS-negative phenotype. The unique requirement of each gene in SLS biosynthesis cannot yet be absolutely confirmed, however, because of the possibility of polar effects. The integrative plasmid pVE6007Δ used for targeted mutagenesis does not contain translational or transcriptional stop signals (52). Moreover, each mutant was constructed with the *cat* gene of pVE6007Δ in the same orientation as the *sag* locus genes, such that transcription initiated from the *cat* promoter may be sufficient to transcribe downstream genes and diminish polar effects. Our RT-PCR results confirm some level of transcription of downstream genes in both the pVE6007Δ and allelic exchange knockouts of *sagA*.

Sequence homologies suggest that SLS is related to the bacteriocin class of antimicrobial peptides. The bacteriocins, including the colicins, microcins, lantibiotics, and nonlantibiotic bacteriocins, typically possess antimicrobial activity against closely related bacterial species and can sometimes exhibit broader hemolytic and cytolytic properties (10, 36). Examples include nisin of *L. lactis* (18), subtilin from *B. subtilis* (3), and the *Enterococcus faecalis* plasmid-encoded hemolysin-bacteriocin (14).

Bacteriocins are synthesized ribosomally as a prepropeptide, comprising an N-terminal leader sequence of 23 to 36 aa and a propeptide of 22 to 60 aa. The propeptide portion then undergoes specific posttranslational modification (e.g., dehydration) of amino acid residues, particularly serine, threonine, and glycine (25). These modified amino acids may then react with a neighboring cysteine residue to produce thioether bridges and unique cyclic structures (40). Following its modification, the prepropeptide is translocated to the cell surface in a process that requires an ABC export complex, at which time the leader peptide is proteolytically cleaved from the mature toxin at a specific sequence site (10).

Examination of *sagA* demonstrates features consistent with a structural gene encoding a bacteriocin-like prepropeptide. In particular, SagA possesses a Gly-Gly sequence motif that is known to immediately precede the cleavage site in several bacteriocins (48). Cleavage at this site would remove a 23-aa leader sequence and leave a 30-aa propeptide with a predicted molecular weight of 2.9 kDa. Koyama (28) calculated the molar ratio of SLS polypeptide to oligonucleotide in highly purified SLS-RNA core preparations to be 0.3. Gel filtration analysis of such preparations yielded a molecular mass of 12.0 kDa for the SLS-oligonucleotide complex, suggesting the polypeptide moiety is approximately $0.3 \times 12{,}000$ to $1.3 \times 12{,}000$ kDa or 2.8 kDa in size (6), which is consistent with the predicted size of the SagA propeptide.

The sequence of the 30-aa SagA propeptide region is unusually rich in threonine (four), serine (five), glycine (six), and cysteine (seven) residues, the precursors for posttranslational modification in several bacteriocin toxins. The presence of such unusual residues may help explain why amino acid analyses of partially purified SLS preparations (2, 28) have differed from the sequence predicted for the SagA propeptide (e.g., absence of cysteine). Previous attempts at sequencing SLS peptide by Edman degradations were unsuccessful (2), which may reflect cyclical thioether bridge structures or N-terminal blockage by a 2-oxobutyryl group as seen in other bacteriocins (35).

Despite the fact that all bacteriocins possess thioether rings and dehydrated residues, there is surprisingly little overall homology pattern among their propeptide sequences (41). SagA propeptide possesses the strongest homology (37% identity, 57% similarity) to McbA, the precursor of microcin B17 of *E. coli*. Microcin B17 is a unique bacteriocin peptide containing posttranslationally modified cysteine, serine, and glycine residues that form directly connected heteroaromatic ring structures (33). The microcin B17 genetic locus includes genes required for chemical modification of prepropeptide amino acids (*mcbB*, *mcbC*, and *mcbD*) and an ABC transporter secretion/immunity apparatus (*mcbE* and *mcbF*). Sequence homology of SagB with McbB, together with its predicted cytoplasmic localization, suggests SagB may be involved in posttranslational modification of amino acid residues in the SLS propeptide.

Bacteriocin peptides are typically exported across the bacterial cytoplasmic membrane by a dedicated ABC transporter (48). The ATP-binding cassette (ABC) transporter complex may sometimes carry out proteolytic processing and removal of the leader peptide concomitant with export of the toxin. Sequence homology indicates that *sagG* to *sagI* encodes the ABC transporter complex of the SLS production pathway, with SagG containing the ABC. It is interesting to speculate that SagG to SagI may also carry out a maturation protease function. Production of functional SLS by GAS has been shown to be inhibited by treatment with protease inhibitors such as tolylsulfonyl phenylalanyl chloromethyl ketone or phenylmethylsulfonyl fluoride, even in the presence of RNA core (1). However, due to relatively small size and lack of a conserved N-terminal segment, SagG itself (and McbF of *E. coli* to which it shares homology) do not appear to belong to the proteolytic GG leader cleaving group of ABC transporters (48).

The homology of SagA bacteriocin-like toxins suggests that SLS may possess antimicrobial activity. Preparations of stabilized SLS are toxic to bacterial protoplasts and spheroplasts (5) but have not to date been shown to inhibit cell-wall-competent bacteria. Certain GAS are known to produce bacteriocins, for example, the lantibiotic streptococcin A from strain FF-22 (24). The GAS M1 genome contains a close homologue of genetic apparatus for the lantibiotic salivaracin A (39). We have performed limited screening of targeted SLS-deficient mutants versus wild-type to probe for antimicrobial activity of the toxin, but we have yet to identify disparities, perhaps due to residual bacteriocin activity attributable to the above-mentioned bacteriocins (data not shown). Identification of potential antimicrobial properties of SLS may require future purification of the mature toxin.

The mechanism(s) whereby bacteriocin-producing bacteria themselves are immune to the antimicrobial effects of the mature toxin are not well understood (41). Genes involved in self-protection have been described in the gene clusters for nisin (29) and subtilin (27) biosynthesis. ABC transporter systems may also participate in bacteriocin immunity, including MbcE to -F of *E. coli* (27). SagE (25.4 kDa) is a possible membrane protein with weak homology to PlnP, a putative *L. plantarum* bacteriocin immunity protein (11). The best sequence match to residues 103 to 179 of SagE in the GenBank database is, in fact, PlnP.

Our discovery of a rho-independent terminator sequence downstream of *sagA* corresponds well with our previously reported 450-bp *sagA* transcript seen by Northern analysis (8). RT-PCR documents the continued presence of *sagA* transcript in downstream SLS-negative mutants (*sagB*.KO to *sagI*.KO),

supporting the hypothesis that SagA requires the action of downstream gene products to become the mature SLS toxin. RT-PCR analysis showed that *sagB* to *-I* is transcribed as a polycistronic message along with *sagA*, but at a level too low for detection by Northern blotting. Thus, the terminator sequence following *sagA* allows some level of read-through. In several bacteriocin gene clusters examined to date, similar gene sequences have been observed downstream of the genes encoding the prebacteriocin, along with mRNA transcripts corresponding to termination at this site (29, 43). This regulatory mechanism, resulting in a differential abundance of mRNAs through leaky termination plus or minus the differential stability of resultant short and long transcripts, appears to be a common feature of bacteriocins (43). GAS may thus generate an excess of the SagA prepropeptide transcript without expending the biochemical resources required to produce equimolar amounts of each gene product in the biosynthesis and export pathway.

Recently, mutagenesis of a GAS response regulator identified as *cov*R increased transcription of *sagA*, along with *hasA* (the first gene of the operon for capsule synthesis), *ska* (streptokinase), and *speMF* (mitogenic factor) (12). Mutagenesis of another two-component GAS regulator, CsR-CsrS, resulted in enhanced transcription of *sagA* and *speB*, the gene encoding pyrogenic exotoxin B (21). Thus, it appears that multiple gene repressor systems may exist for SLS and other potential GAS virulence factors. It is also possible that SLS itself is involved in GAS regulatory networks, as increased *sagA* expression from an inducible plasmid resulted in increased message levels for M protein (*emm*) in an M49 parent strain (32).

In summary, we have discovered and characterized by targeted mutagenesis, complementation, and heterologous expression a nine-gene operon required for SLS production by GAS. The *sag* operon is headed by a candidate gene for a bacteriocin prepropeptide, SagA, the likely SLS precursor. The *sag* operon also contains candidate genes for chemical modification of the bacteriocin propeptide and self protection, an ABC transporter for export and maturation proteolysis of the leader peptide, and an internal terminator motif for differential transcription of structural gene and accessory gene mRNAs. We have previously demonstrated the significance of SLS as a virulence determinant in an animal model of necrotic skin infection (8). The targeted isogenic SLS-negative mutants we have created will allow further study of cytotoxic properties of this molecule and its role in disease pathogenesis. In addition, the expression of SLS in a hemolysin-negative heterologous host will facilitate attempts at purification of the recombinant toxin, determination of its chemical structure, and elucidation of its mechanism of action.

ACKNOWLEDGMENTS

This work was supported by NIH/NIAID grant AI 01451 (V.N.) and the Canadian Bacterial Diseases Network (J.D.A. and D.E.L.). D.J.B. is a recipient of the Medical Research Council of Canada Postdoctoral Research Fellowship.

We thank Craig Pritzlaff for his assistance in primer selection.

REFERENCES

1. **Akao, T., K. Kobashi, and C. Y. Lai.** 1983. The role of protease in streptolysin S formation. Arch. Biochem. Biophys. **223:**556–561.
2. **Alouf, J. E., and C. Loridan.** 1988. Production, purification, and assay of streptolysin S. Methods Enzymol. **165:**59–64.
3. **Banerjee, S., and J. N. Hansen.** 1988. Structure and expression of a gene encoding the precursor of subtilin, a small protein antibiotic. J. Biol. Chem. **263:**9508–9514.
4. **Beall, B., R. R. Facklam, J. A. Elliott, A. R. Franklin, T. Hoenes, D. Jackson, L. Laclaire, T. Thompson, and R. Viswanathan.** 1998. Streptococcal emm types associated with T-agglutination types and the use of conserved emm gene restriction fragment patterns for subtyping group A streptococci. J. Med. Microbiol. **47:**893–898.
5. **Bernheimer, A. W.** 1966. Disruption of wall-less bacteria by streptococcal and staphylococcal toxins. J. Bacteriol. **91:**1677–1680.
6. **Bernheimer, A. W.** 1967. Physical behavior of streptolysin S. J. Bacteriol. **93:** 2024–2025.
7. **Bernheimer, A. W., and L. L. Schwartz.** 1964. Lysosomal disruption by bacterial toxins. J. Bacteriol. **87:**1100–1104.
8. **Betschel, S. D., S. M. Borgia, N. L. Barg, D. E. Low, and J. C. De Azavedo.** 1998. Reduced virulence of group A streptococcal Tn*916* mutants that do not produce streptolysin S. Infect. Immun. **66:**1671–1679.
9. **Chaffin, D. O., and C. E. Rubens.** 1998. Blue/white screening of recombinant plasmids in Gram-positive bacteria by interruption of alkaline phosphatase gene (*phoZ*) expression. Gene **219:**91–99.
10. **de Vos, W. M., O. P. Kuipers, J. R. van der Meer, and R. J. Siezen.** 1995. Maturation pathway of nisin and other lantibiotics: post-translationally modified antimicrobial peptides exported by Gram-positive bacteria. Mol. Microbiol. **17:**427–437.
11. **Diep, D. B., L. S. Havarstein, and I. F. Nes.** 1996. Characterization of the locus responsible for the bacteriocin production in *Lactobacillus plantarum* C11. J. Bacteriol. **178:**4472–4483.
12. **Federle, M. J., K. S. McIver, and J. R. Scott.** 1999. A response regulator that represses transcription of several virulence operons in the group A streptococcus. J. Bacteriol. **181:**3649–3657.
13. **Framson, P. E., A. Nittayajarn, J. Merry, P. Youngman, and C. E. Rubens.** 1997. New genetic techniques for group B streptococci: high-efficiency transformation, maintenance of temperature-sensitive pWV01 plasmids, and mutagenesis with Tn*917*. Appl. Environ. Microbiol. **63:**3539–3547.
14. **Gilmore, M. S., R. A. Segarra, M. C. Booth, C. P. Bogie, L. R. Hall, and D. B. Clewell.** 1994. Genetic structure of the *Enterococcus faecalis* plasmid pAD1-encoded cytolytic toxin system and its relationship to lantibiotic determinants. J. Bacteriol. **176:**7335–7344.
15. **Ginsburg, I.** 1972. Mechanisms of cell and tissue injury induced by group A streptococci: relation to poststreptococcal sequelae. J. Infect. Dis. **126:**294–340.
16. **Ginsburg, I.** 1970. Streptolysin S, p. 99–176. *In* T. C. Montie, S. Kadis, and S. J. Ajl (ed.), Microbial toxins, vol. 3. Bacterial protein toxins. Academic Press, Inc., New York, N.Y.
17. **Grant, S. G., J. Jessee, F. R. Bloom, and D. Hanahan.** 1990. Differential plasmid rescue from transgenic mouse DNAs into Escherichia coli methylation-restriction mutants. Proc. Natl. Acad. Sci. USA **87:**4645–4649.
18. **Gross, E., and J. L. Morell.** 1971. The structure of nisin. J. Am. Chem. Soc. **93:**4634–4635.
19. **Gupta, A.** 1999. RT-PCR: characterization of long multi-gene operons and multiple transcript gene clusters in bacteria. BioTechniques **27:**966–970, 972.
20. **Gutierrez, J. A., P. J. Crowley, D. P. Brown, J. D. Hillman, P. Youngman, and A. S. Bleiweis.** 1996. Insertional mutagenesis and recovery of interrupted genes of *Streptococcus mutans* by using transposon Tn*917*: preliminary characterization of mutants displaying acid sensitivity and nutritional requirements. J. Bacteriol. **178:**4166–4175.
21. **Heath, A., V. J. DiRita, N. L. Barg, and N. C. Engleberg.** 1999. A two-component regulatory system, CsrR-CsrS, represses expression of three *Streptococcus pyogenes* virulence factors, hyaluronic acid capsule, streptolysin S, and pyrogenic exotoxin B. Infect. Immun. **67:**5298–5305.
22. **Holo, H., and I. F. Nes.** 1989. High-frequency transformation, by electroporation, of *Lactococcus lactis* subsp. *cremoris* grown with glycine in osmotically stabilized media. Appl. Environ. Microbiol. **55:**3119–3123.
23. **Hryniewicz, W., and J. Pryjma.** 1977. Effect of streptolysin S on human and mouse T and B lymphocytes. Infect. Immun. **16:**730–733.
24. **Jack, R. W., A. Carne, J. Metzger, S. Stefanovic, H. G. Sahl, G. Jung, and J. Tagg.** 1994. Elucidation of the structure of SA-FF22, a lanthionine-containing antibacterial peptide produced by *Streptococcus pyogenes* strain FF22. Eur. J. Biochem. **220:**455–462.
25. **Jung, G.** 1991. Lantibiotics—ribosomally synthesized biologically active polypeptides containing sulfide bridges and α,β-didehydroamino acids. Angew. Chem. Int. Ed. Engl. **30:**1051–1192.
26. **Keiser, H., G. Weissmann, and A. W. Bernheimer.** 1964. Studies on lysosomes. IV. Solubilization of enzymes during mitochondrial swelling and disruption of lysosomes by streptolysins and other hemolytic agents. J. Cell Biol. **22:**101.
27. **Klein, C., and K. D. Entian.** 1994. Genes involved in self-protection against the lantibiotic subtilin produced by *Bacillus subtilis* ATCC 6633. Appl. Environ. Microbiol. **60:**2793–2801.
28. **Koyama, J.** 1963. Biochemical studies on streptolysin S. II. Properties of a polypeptide component and its role in the toxin activity. J. Biochem. **54:** 146–151.
29. **Kuipers, O. P., M. M. Beerthuyzen, R. J. Siezen, and W. M. De Vos.** 1993. Characterization of the nisin gene cluster nisABTCIPR of *Lactococcus lactis*. Requirement of expression of the *nis*A and *nis*I genes for development of immunity. Eur. J. Biochem. **216:**281–291.
30. **Kuipers, O. P., P. G. G. A. de Ruyter, M. Kleerebezem, and W. M. de Vos.**

1998. Quorum sensing-controlled gene expression in lactic acid bacteria. J. Biotechnol. **64:**15–21.
31. **Kuypers, J. M., L. M. Heggen, and C. E. Rubens.** 1989. Molecular analysis of a region of the group B streptococcus chromosome involved in type III capsule expression. Infect. Immun. **57:**3058–3065.
32. **Li, Z., D. D. Sledjeski, B. Kreikemeyer, A. Podbielski, and M. D. Boyle.** 1999. Identification of *pel*, a *Streptococcus pyogenes* locus that affects both surface and secreted proteins. J. Bacteriol. **181:**6019–6027.
33. **Madison, L. L., E. I. Vivas, Y. M. Li, C. T. Walsh, and R. Kolter.** 1997. The leader peptide is essential for the post-translational modification of the DNA-gyrase inhibitor microcin B17. Mol. Microbiol. **23:**161–168.
34. **Maguin, E., P. Duwat, T. Hege, D. Ehrlich, and A. Gruss.** 1992. New thermosensitive plasmid for gram-positive bacteria. J. Bacteriol. **174:**5633–5638.
35. **Meyer, H. E., M. Heber, B. Eisermann, H. Korte, J. W. Metzger, and G. Jung.** 1994. Sequence analysis of lantibiotics: chemical derivatization procedures allow a fast access to complete Edman degradation. Anal. Biochem. **223:**185–190.
36. **Nes, I. F., and J. R. Tagg.** 1996. Novel lantibiotics and their pre-peptides. Antonie Leeuwenhoek. **69:**89–97.
37. **Podbielski, A., B. Spellerberg, M. Woischnik, B. Pohl, and R. Lutticken.** 1996. Novel series of plasmid vectors for gene inactivation and expression analysis in group A streptococci (GAS). Gene **177:**137–147.
38. **Rose, R. E.** 1988. The nucleotide sequence of pACYC184. Nucleic Acids Res. **16:**355.
39. **Ross, K. F., C. W. Ronson, and J. R. Tagg.** 1993. Isolation and characterization of the lantibiotic salivaricin A and its structural gene *salA* from *Streptococcus salivarius* 20P3. Appl. Environ. Microbiol. **59:**2014–2021.
40. **Sahl, H. G., and G. Bierbaum.** 1998. Lantibiotics: biosynthesis and biological activities of uniquely modified peptides from gram-positive bacteria. Annu. Rev. Microbiol. **52:**41–79.
41. **Siezen, R. J., O. P. Kuipers, and W. M. de Vos.** 1996. Comparison of lantibiotic gene clusters and encoded proteins. Antonie Leeuwenhoek. **69:** 171–184.
42. **Simon, D., and J. J. Ferretti.** 1991. Electrotransformation of *Streptococcus pyogenes* with plasmid and linear DNA. FEMS Microbiol. Lett. **66:**219–224.
43. **Skaugen, M., C. I. Abildgaard, and I. F. Nes.** 1997. Organization and expression of a gene cluster involved in the biosynthesis of the lantibiotic lactocin S. Mol. Gen. Genet. **253:**674–686.
44. **Stevens, D. L.** 1999. The flesh-eating bacterium: what's next? J. Infect. Dis. **179**(Suppl. 2)**:**366–374.
45. **Stingele, F., S. J. Vincent, E. J. Faber, J. W. Newell, J. P. Kamerling, and J. R. Neeser.** 1999. Introduction of the exopolysaccharide gene cluster from *Streptococcus thermophilus* Sfi6 into *Lactococcus lactis* MG1363: production and characterization of an altered polysaccharide. Mol. Microbiol. **32:**1287–1295.
46. **Taketo, Y., and A. Taketo.** 1966. Cytolytic effect of streptolysin S complex on Ehrlich ascites tumor cells. J. Biochem. (Tokyo) **60:**357–362.
47. **Theodore, T. S., and G. B. Calandra.** 1981. Streptolysin S activation by lipoteichoic acid. Infect. Immun. **33:**326–328.
48. **van Belkum, M. J., R. W. Worobo, and M. E. Stiles.** 1997. Double-glycine-type leader peptides direct secretion of bacteriocins by ABC transporters: colicin V secretion in *Lactococcus lactis*. Mol. Microbiol. **23:**1293–1301.
49. **Walker, J. E., M. Saraste, M. J. Runswick, and N. J. Gay.** 1982. Distantly related sequences in the alpha- and beta-subunits of ATP synthase, myosin, kinases and other ATP-requiring enzymes and a common nucleotide binding fold. EMBO J. **1:**945–951.
50. **Woodcock, D. M., P. J. Crowther, J. Doherty, S. Jefferson, E. DeCruz, M. Noyer-Weidner, S. S. Smith, M. Z. Michael, and M. W. Graham.** 1989. Quantitative evaluation of *Escherichia coli* host strains for tolerance to cytosine methylation in plasmid and phage recombinants. Nucleic Acids Res. **17:**3469–3478.
51. **Yamamoto, H., S. Uchiyama, and J. Sekiguchi.** 1996. The *Bacillus subtilis* chromosome region near 78 degrees contains the genes encoding a new two-component system, three ABC transporters and a lipase. Gene **181:** 147–151.
52. **Yim, H. H., and C. E. Rubens.** 1998. Site-specific homologous recombination mutagenesis in group B streptococci. Methods Cell Sci. **20:**13–20.
53. **Yorgey, P., J. Davagnino, and R. Kolter.** 1993. The maturation pathway of microcin B17, a peptide inhibitor of DNA gyrase. Mol. Microbiol. **9:**897–905.

Editor: E. I. Tuomanen